

## Small-Angle Neutron Scattering of Blends of Arborescent Polystyrenes

Sangwook Choi and Robert M. Briber\*

*Department of Materials and Nuclear Engineering, University of Maryland, College Park, Maryland 20742-7531*

Barry J. Bauer and Da-Wei Liu

*Polymers Division, National Institute of Standards and Technology, Gaithersburg, Maryland 20899-8542*

Mario Gauthier

*Institute for Polymer Research, Department of Chemistry, University of Waterloo, Waterloo, Ontario N2L 3G1, Canada**Received January 31, 2000; Revised Manuscript Received June 1, 2000*

**ABSTRACT:** Small-angle neutron scattering (SANS) was used to measure the size and shape of styrene-based arborescent polymers blended with linear deuterated polystyrene (d-PS) and linear deuterated poly(vinyl methyl ether) (d-PVME). For generation 0, 1, and 2 arborescent polymers, the  $R_g$  were essentially equivalent in going from d-PVME to d-PS as the matrix material while for generation 3 (G3) the  $R_g$  in d-PS was found to be smaller than in d-PVME. For comparison, the  $R_g$  of a sphere was calculated assuming the size of the sphere was equivalent to a G3 molecule collapsed to bulk density. The  $R_g$  obtained was 162 Å, which is quite close to the  $R_g$  of the G3 polymer in d-PS ( $R_g = 164$  Å). This indicates that the G3 molecules should behave as essentially noninterpenetrating spheres with the linear d-PS matrix chains being largely excluded from the interior of the arborescent molecules. In the single phase region of the phase diagram it was difficult to establish a clear temperature dependence of the  $R_g$  for the generation 0, 1, and 2 molecules in d-PVME. For the G3 molecules in d-PVME a small decrease in  $R_g$  with increasing temperature was observed in the single phase region with an abrupt decrease of 21% on phase separation between 110 and 115 °C. The single particle form factor of arborescent polymers in blends was studied using a power law model for the density profile. In comparison with a hard sphere or a shell model, the scattering function calculated from the power law function for the density profile provided the best fit to the experimental scattering data.

## Introduction

Various types of dendritic polymers with controlled architecture such as dendrimers, hyperbranched polymers, and arborescent polymers have been developed recently.<sup>1–13</sup> This special class of branched polymers has gained increasing interest from both theoretical and practical points of view. For example, they can be used as cross-linking agents, sensors, catalysts, size standards, and drug release systems.<sup>2,14,15</sup> For many applications it is necessary to have detailed information on the intramolecular density profile, molecular size, and shape in solution and in mixtures with other polymers.

Arborescent polymers are branched macromolecules synthesized by successive cycles of functionalization and grafting reactions.<sup>7–13</sup> The structure of arborescent polymers is represented schematically in Figure 1. The structure of arborescent polymers has features distinct from the classical dendrimer molecules. The building blocks used in the synthesis of arborescent polymers are polymer chains rather than small molecules. The grafting sites in arborescent polymer molecules are randomly distributed, rather than strictly controlled like in dendrimer molecules. In our previous paper the size of arborescent polystyrenes in solution was measured as a function of temperature and molecular mass using small-angle neutron scattering (SANS).<sup>16</sup> In this paper small-angle neutron scattering is used to study arborescent polystyrenes in blends with linear polymers for comparison to the results obtained in solutions. Deu-

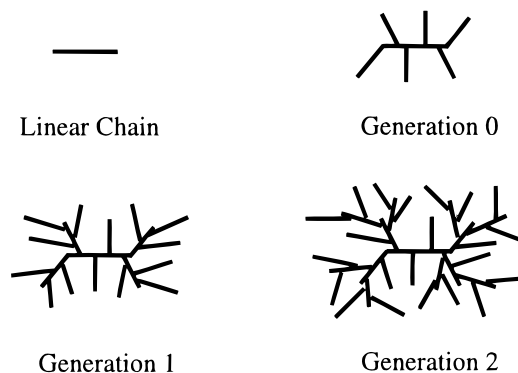


**Figure 1.** Schematic representation of the growth of arborescent polymers by successive grafting reactions.

terated polystyrene (d-PS) and deuterated PVME (d-PVME) are used as matrix polymers to study arborescent polymer blends as a function of molecular mass and temperature.

According to classical Flory theory for a linear polymer chain in a good and a  $\Theta$  solvent, the scaling exponent for  $R_g \sim M^{\nu}$  is 0.6 and 0.5, respectively, where  $R_g$  is the radius of gyration and  $M$  is the molecular mass (or chain length). Linear polymer chains are fractal objects, which means that as the molecular mass of a linear polymer chain increases, the average density of the linear chain decreases. The density is taken as an average coil density estimated as  $\rho \sim M/R_g^3$ .<sup>17</sup> In the work by Zimm and Stockmayer, who studied this scaling

relation for branched polymers, the scaling exponent was found to be 0.25 for a Cayley tree in the limit of large molecular mass. This value of the scaling exponent is smaller than the value of  $1/3$  for a constant density object, which means that as the size of a (highly) branched polymer increases, the (average coil) density of the branched polymer increases.<sup>18</sup> de Gennes and Hervet studied the scaling relation for dendrimers using an analytical calculation, and the scaling exponent was found to be 0.2.<sup>19</sup> Stauffer et al. studied the scaling relation for branched polymers taking into account the excluded-volume effect and compared their results with the classical theory given by Flory and Stockmayer.<sup>20–22</sup> They showed that the limiting exponent for the size of the gel particles with molecular weight has to be at least  $1/3$  based on density considerations. According to numerous computer simulations and limited experimental work on dendrimers, the values of this scaling exponent have been reported in the range of 0.2–0.4.<sup>23–27</sup> It should be noted that any value of the scaling exponent less than  $1/3$  has physical limitations and cannot be maintained as  $M \rightarrow \infty$ , due to density constraints. In our previous work on arborescent polymers in solution, the scaling exponent was found to be  $\nu = 0.25 \pm 0.01$  in deuterated cyclohexane and  $\nu = 0.32 \pm 0.01$  in deuterated toluene.<sup>16</sup> These values of  $\nu$  are less than  $1/3$ , indicating again that the average segment density in the polymer coil is increasing with increasing molecular weight. This creates a self-limiting condition where the coil density approaches bulk density, and arborescent polymers of higher generations can no longer be synthesized with a constant branching density.

The intramolecular radial density profile of dendrimer molecules proposed by de Gennes and Hervet has a minimum density at the center of the molecule.<sup>19</sup> However, a number of computer simulations<sup>24–27</sup> and theoretical work by Boris and Rubinstein<sup>28</sup> predict a maximum in the radial density profile at the center of the molecule and a decreasing density gradient to the outer edge of the molecule. According to recent small-angle X-ray scattering (SAXS) work, generation 10 polyamidoamine (PAMAM) dendrimers in solution do not exhibit any sizable minimum in density near the core.<sup>29</sup> More recent results by Prosa et al. show that the dendrimers exhibit spherelike characteristics.<sup>30</sup> According to recent small-angle neutron scattering (SANS) work by Pötschke et al., the density for a dendrimer in solution has a maximum at the center of the molecules.<sup>31</sup> In our previous work on arborescent polymer in solutions, a power law model for the radial density profile which has a maximum density at the center of molecule was used to successfully model the single particle form factor.<sup>16</sup> This function has a relatively constant interior density and an outer zone of transition that is dependent on the solvent used.

## Experimental Section

The arborescent polymers used in this study were synthesized by successive grafting reactions of polystyryl anions onto a linear polystyrene substrate.<sup>12</sup> The molecular mass of the branches used for grafting for each generation was determined by gel permeation chromatography (GPC). The molecular mass of the arborescent polymers was not determined by GPC but was measured in this work as part of the SANS analysis. The characteristics of the arborescent polymers used in the study and the branches are given in Table 1. Molecular mass of the branches from GPC is  $\pm 10\%$  as is typical of this technique. The core and the side chains used in the synthesis of each

**Table 1. Characteristics of Arborescent Polymers with 5000 g mol<sup>-1</sup> Branches**

generation	branches		graft polymer		
	$M_w/10^3$ g mol <sup>-1</sup>	$M_w/M_n$	$M_w$ g mol <sup>-1</sup>	$f_w(\text{tot})$	branching density
0	4.3	1.03	$5.7 \times 10^4$	12	0.25
1	4.6	1.03	$5.7 \times 10^5$	120	0.20
2	4.2	1.04	$3.2 \times 10^6$	720	0.11
3	4.4	1.05	$2.4 \times 10^7$	5200	0.15

**Table 2. Characteristics of Deuterated Polystyrene and Deuterated Poly(vinyl methyl ether) g mol<sup>-1</sup>**

	$M_w/M_n$	$M_w$	$M_n$
d-PS	1.03	4 300	4 170
	1.03	26 600	25 800
	1.51	102 900	68 100
	1.04	244 000	235 000
d-PVME	1.05	424 900	404 700
	2.05	8 280	4 040

generation had a molecular mass of around 5000 g/mol. The total number of branches in a given generation  $G$  polymer was calculated using eq 1:

$$f_w(\text{tot}) = f_w(G-1) + \frac{M_w(G) - M_w(G-1)}{M_w(\text{branch})} \quad (1)$$

where  $M_w(G)$ ,  $M_w(G-1)$ , and  $M_w(\text{branch})$  are the molecular masses of a generation  $G$  polymer, of the previous generation, and of the grafted side chains, respectively. If the molecular mass of the branches for all generations is the same, eq 1 can be reduced to a simpler form:

$$f_w(\text{tot}) = \frac{M_w(G) - M_w(\text{linear core})}{M_w(\text{branch})} \quad (2)$$

The branching density of the core portion of a generation  $G$  polymer is given by eq 3:

$$\text{branching density} = \frac{\text{no. of branches added per molecule in a grafting reaction}}{\text{total no. of repeat units of previous generation}} \quad (3)$$

Blends of the arborescent and linear polymers were prepared using deuterated linear polystyrene or deuterated linear poly(vinyl methyl ether). The deuterated linear polystyrene samples were either purchased or synthesized, depending on the molecular mass. Deuterated styrene purchased from Cambridge Isotope Laboratories, Inc., and a tetramethylpiperidinyloxy (TEMPO)-based unimolecular initiator obtained from Dr. C. Hawker at the IBM Almaden Research Center were used to synthesize deuterated linear polystyrene by living free radical polymerization.<sup>32,33</sup> Deuterated linear PVME was synthesized by cationic polymerization of  $d_3$ -vinyl methyl ether,  $\text{CH}_2=\text{CHOCD}_3$ , in toluene using the boron trifluoride-ethyl ether complex as the initiator.<sup>34,35</sup> The molecular masses of deuterated polystyrene and deuterated PVME were determined using GPC, and the mass average molecular masses were found to be 102 900 and 8280 g/mol, respectively. Universal calibration was used with the Mark-Houwink-Sakurada parameters  $a = 0.739$  and  $k = 1.35 \times 10^{-4}$  for d-PVME in tetrahydrofuran (THF) at 30 °C.<sup>34,35</sup> In addition to the deuterated polystyrene synthesized by living free radical polymerization, several anionically polymerized deuterated polystyrenes of different molecular masses were purchased from Polymer Laboratories, Ltd. The characteristics of the linear polymers are summarized in Table 2. Samples for neutron scattering were prepared by dissolving the appropriate deuterated linear polymer and the arborescent polymer in toluene and then allowing the solution to evaporate in a Teflon Petri dish to form a thin film. The film was then dried in a

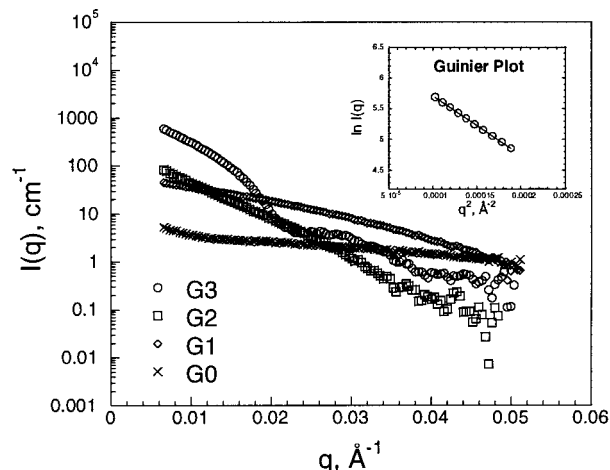


**Figure 2.** SANS curves for all arborescent polymer generations in d-polystyrene at 120 °C.

vacuum to remove any remaining toluene. The film was pressed into a disk of 1.4 cm in diameter and 0.05 cm in thickness for the SANS experiments using a hot press at approximately 150 °C. The concentration range of the blends studied was  $\phi = 0.5\text{--}2\%$ , mass fraction of the arborescent polymer.

Small-angle neutron scattering experiments were carried out using the 30 m NIST-NG3 instrument at the Center for Neutron Research of the National Institute of Standards and Technology.<sup>36,37</sup> The raw data were corrected for scattering from the empty cell, incoherent scattering, detector dark current, detector sensitivity, sample transmission, and thickness. Following these corrections the data were placed on an absolute scale using a calibrated secondary standard and circularly averaged to produce  $I(q)$  versus  $q$  plots where  $I(q)$  is the scattered intensity and  $q$  is the scattering vector. The  $q$  range was from 0.0046 to 0.0520  $\text{\AA}^{-1}$  with a neutron wavelength,  $\lambda = 6 \text{ \AA}$ , and a wavelength spread,  $\Delta\lambda/\lambda = 0.15$ .

The uncertainties reported are calculated as the estimated standard deviation of the mean. The total combined uncertainty is not given, as comparisons are made only with data obtained under the same conditions. In cases where the limits are smaller than the plotted symbols, the limits are left out for clarity. Fits of the scattering data are made by a least-squares fit to the data giving an average and a standard deviation to the fit. All temperatures reported are within  $\pm 1$  °C as determined by previous calibration.

## Results and Discussion

A typical set of SANS data for all generations ( $T = 120$  °C,  $\phi = 1\%$  in deuterated polystyrene) is shown in Figure 2. The radii of gyration were measured using Guinier plots at small  $q$  as given by eq 4:

$$I(q) = I(0) \exp\left(-\frac{R_g^2 q^2}{3}\right) \quad (4)$$

where  $R_g$  is the radius of gyration of the object.<sup>38,39</sup> A typical Guinier plot of  $\ln I(q)$  versus  $q^2$  for a generation 3 (G3) polymer is displayed as an inset in Figure 2. The  $R_g$  of the arborescent polymer molecules in blends was plotted as a function of generation number (molecular mass) and compared with data from solutions measured previously in Figure 3.<sup>16</sup> The error bars in Figure 3 represent one standard deviation calculated from the linear least-squares fit of the Guinier plot data. The  $R_g$  decreases in going from solutions to blends, and the observed  $R_g$  is smaller in linear deuterated polystyrene than in deuterated PVME. (Note that the molecular masses of the two linear polymers are quite different

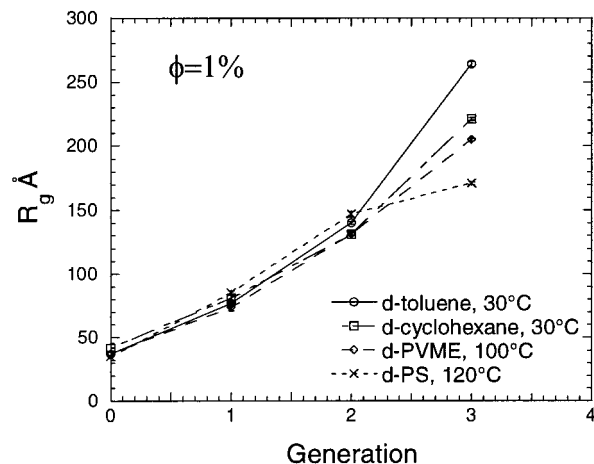


**Figure 3.**  $R_g$  of arborescent polymers in solutions and in blends as a function of generation number.

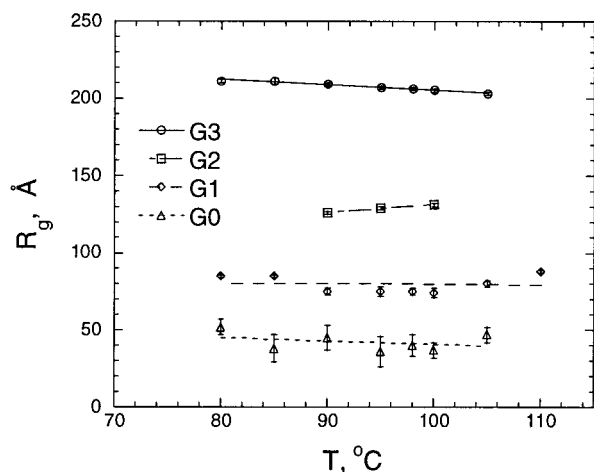


**Figure 4.** Temperature dependence of  $R_g$  for arborescent polymers in d-PVME.

at 103K and 8.2K, respectively.) As will be discussed in detail later in the paper, the  $R_g$  of the G3 polymer was also studied as a function of the molecular mass of the d-PS matrix polymer. The  $R_g$  of the G3 polymer in d-PS with  $N = 38$  ( $M_w = 4.3\text{K}$ ) and  $N = 238$  ( $M_w = 27\text{K}$ ) was found to be 206 and 182  $\text{\AA}$ , respectively, while  $R_g$  in d-PVME with  $N = 131$  ( $M_w = 8.2\text{K}$ ) was 205  $\text{\AA}$  ( $N$  is the average number of monomer units in the chains). Although the d-PVME chain length falls between the two d-PS molecular masses studied, it appears that for equivalent chain lengths the  $R_g$  would be smaller with d-PS as the matrix.

The radii of gyration for the arborescent polymers in d-PVME are plotted as a function of temperature in Figure 4. Polystyrene/poly(vinyl methyl ether) blends are well-known to exhibit a lower critical solution temperature (LCST) type phase diagram with a critical point between 110 and 160 °C depending on molecular mass and deuteration effects.<sup>40–42</sup> The polystyrene/poly(vinyl methyl ether) blends studied in this work contain deuterated PVME. All previous neutron scattering work on PS/PVME blends used polystyrene as the deuterated component. All the data in Figure 4 are from blends in the single phase region of the phase diagram. It is difficult to interpret the data in Figure 4 in terms of any systematic temperature dependence of  $R_g$  in the single phase region of the phase diagram. The temperature dependence of  $R_g$  for arborescent polymers in d-PS was not studied.

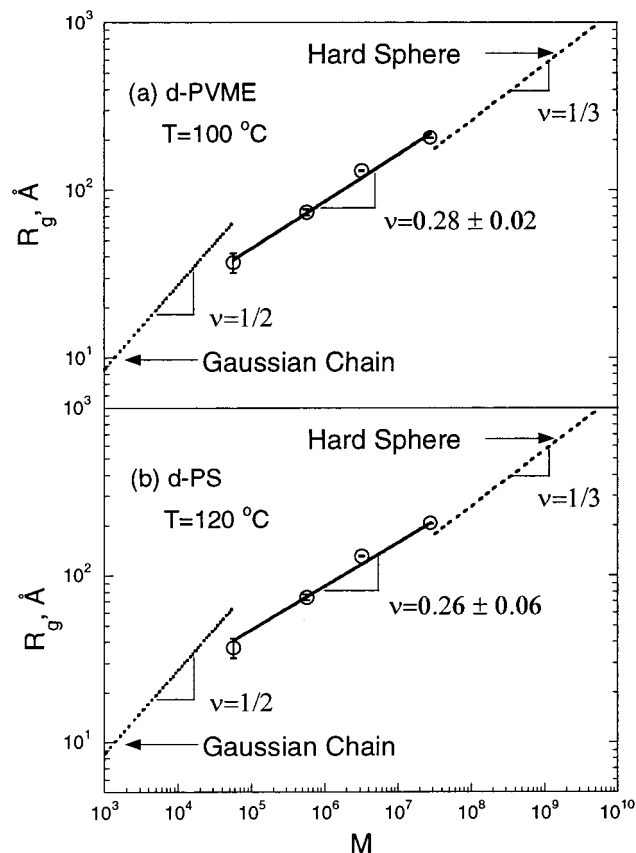


**Figure 5.** (a)  $R_g$  versus molecular mass for arborescent polymers in d-PVME. (b)  $R_g$  versus molecular mass for arborescent polymers in d-polystyrene.

A scaling relation given by  $R_g = kM^\nu$  exists between the  $R_g$  and the molecular mass,  $M_w$ , where  $\nu$  is the scaling factor and  $k$  is a constant. The log–log plots of  $R_g$  versus  $M$  for the arborescent polymers in d-PVME and d-PS are shown in Figure 5a,b. Two dashed lines are shown in Figure 5a,b: one calculated for a Gaussian linear polystyrene chain and the other for a sphere with the bulk density of polystyrene, assuming the chain is completely collapsed. As observed in previous work on arborescent polymers in solution, the arborescent polymers exhibit a crossover between a Gaussian linear chain ( $\nu = 1/2$ ) and an object with constant density ( $\nu = 1/3$ ).<sup>16</sup> The exponent of  $\nu$  for the arborescent polymers in d-PVME and d-PS was found to be  $\nu = 0.28 \pm 0.02$  and  $\nu = 0.26 \pm 0.06$ , respectively, which indicates that the average polymer segment density inside the sphere defined by the  $R_g$  increases with increasing generation.

A power law function for the radial density was used to calculate the expected scattering and fit to the SANS data for the G3 polymer. The fitting procedures and uncertainties are reported elsewhere.<sup>43</sup> The fit was optimized by varying the value of  $\alpha$ . The power law function is given by

$$\rho(r) = 1 - \left(\frac{r}{R_{\max}}\right)^\alpha \quad (5)$$

where  $R_{\max}$  corresponds to the hydrodynamic radius. The scattering was calculated using eq 6.<sup>41,44</sup>

$$I(q) \propto \left[ \int dr \rho(r) \frac{\sin(qr)}{qr} r^2 \right]^2 \quad (6)$$

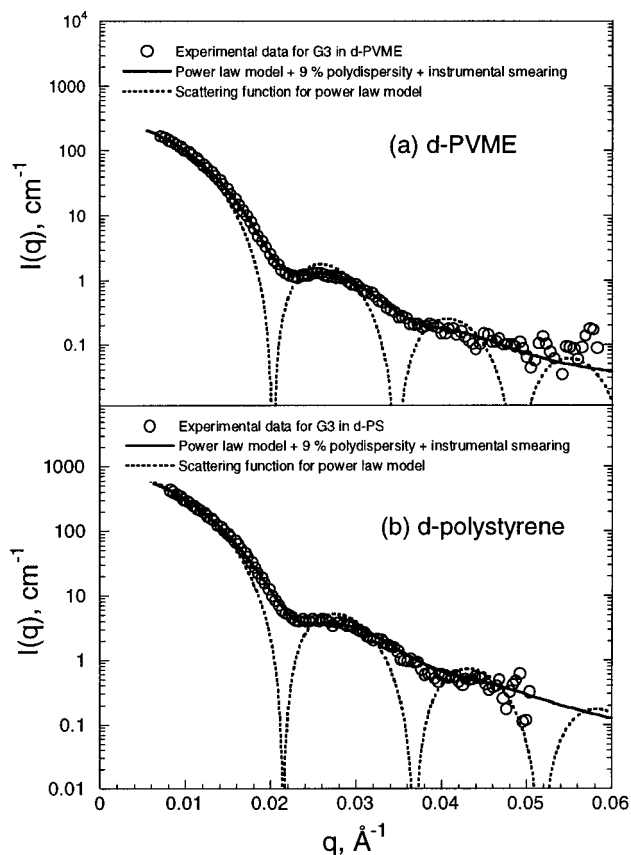


**Figure 6.** (a) Scattering functions for power law model compared with G3 polymer in d-PVME. (b) Scattering functions for power law model compared with G3 polymer in d-polystyrene.

The best fit to the SANS data for the G3 molecule was found when  $\alpha = 12$  and  $\alpha = 18$  for d-PVME and d-PS, respectively, and the fits to the scattering data are shown in Figure 6a,b. The fits to the data in Figure 6a,b include a 9% polydispersity of the polymer and the effect of instrumental smearing with  $I(0)$ ,  $R_{\max}$ , and a baseline as floating parameters.<sup>45–48</sup> The values of  $R_{\max} = 260 \pm 4 \text{ \AA}$  and  $R_{\max} = 221 \pm 4 \text{ \AA}$  were obtained from the fit to the scattering data in Figure 6a,b for the G3 polymer in d-PVME and d-PS, respectively. The error bars for the values of  $R_{\max}$  were calculated from the errors in  $q$  based on the SANS instrument configuration. A comparison of the radial density profiles in blends with those obtained from previous work on G3 arborescent polystyrenes in solutions is shown in Figure 7.<sup>16</sup> The density profile for arborescent polymers in blends with linear chains decreases more rapidly at the outside edge of molecules in comparison with that in solutions ( $\alpha = 4$ ). The density profile of arborescent polymers in d-PS is close to that of a hard sphere. Using the power law density function given by eq 5, the radius of gyration can be calculated from eq 7.

$$R_g^2 = \frac{\int dr \rho(r) r^4}{\int dr \rho(r) r^2} \quad (7)$$

The relation between  $R_g$  and  $R_{\max}$  for arborescent polymers in d-PS was found to be  $R_g = (63/115)^{1/2} R_{\max}$  (for  $\alpha = 18$ ), and the calculated  $R_g$  was 164 Å. For comparison, the  $R_g$  of a sphere was calculated assuming that the G3 molecules were collapsed to the bulk

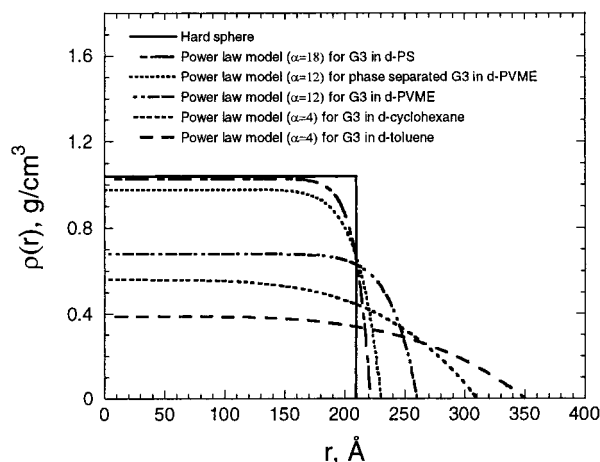


**Figure 7.** Density profiles for G3 arborescent polymer in solutions and blends.

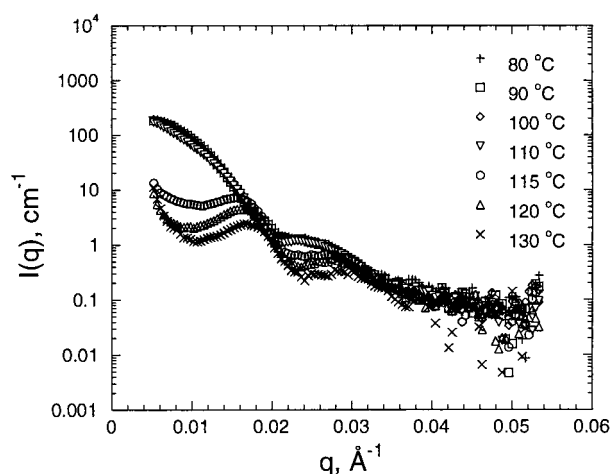


**Figure 8.**  $I(q)$  versus  $q$  for G3 polymer in d-PVME from 80 °C to the phase separation temperature.

density. The  $R_g$  obtained was approximately 162 Å, which is close to the  $R_g$  of the G3 polymer in d-PS. This indicates that the G3 molecules in d-PS should be noninterpenetrating, and the linear d-PS is largely excluded from the interior of the arborescent molecules.

The measured scattering from the G3 in deuterated poly(vinyl methyl ether) (PVME) was essentially constant as the temperature was changed from 80 to 105 °C. No increase in the concentration fluctuation scattering was observed as the phase separation was approached, as is typically observed for polymer blends.<sup>48–50</sup> Phase separation occurs above 110 °C, and two peaks develop as shown in Figure 8. Upon phase separation, the single particle form factor peak (the second peak located at  $q = 0.023 \text{ \AA}^{-1}$ ) shifts to higher  $q$ , indicating that the size of the molecules decreased. The size of the molecules after phase separation was estimated from the position of the second form factor peak using the power law model and plotted as a function of temperature in Figure 9. As noted previously, there is no appreciable temperature dependence of  $R_g$  in the single phase region, but a collapse of the G3 molecules by about 21% is observed with phase separation. The collapse transition has long been of interest and has generated much theoretical and experimental work, because of its relevance to local polymer structure, fractionation, and biological applications such as protein folding.<sup>51,52</sup> To the authors' best knowledge, this is the first direct observation of a collapse transition observed

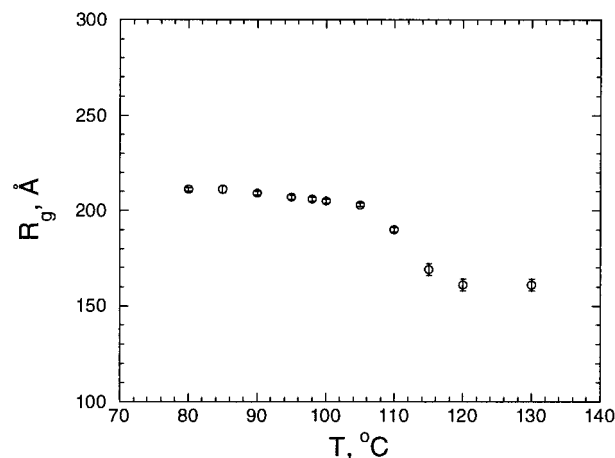


**Figure 9.** Temperature dependence of  $R_g$  for G3 polymer in d-PVME.

in polymer blends, although it has been predicted in simulations<sup>53</sup> and theoretically.<sup>54</sup> It should also be noted that d-PVME is of quite low molecular mass. The variation in the size of a linear polystyrene chain in cyclohexane as a function of temperature near the  $\Theta$  temperature has been studied by many authors, and the collapse transition for a linear chain in deuterated cyclohexane has been observed below the  $\Theta$  temperature.<sup>51,52,55–59</sup> In our previous experiments on arborescent polymers in deuterated cyclohexane, the radius of gyration decreased by 15% when phase separation occurred.<sup>16</sup> At 115 °C two peaks are found in the  $I(q)$  versus  $q$  data for the G3 in deuterated poly(vinyl methyl ether). The first peak is due to the interference between molecules, while the second peak arises from the single particle form factor. The scattering intensity for a particulate system can be expressed as<sup>29,41,60</sup>

$$I(q) = k_n NP(q) S(q) \quad (8)$$

where  $k_n$  is the contrast factor for neutrons,  $N$  is the concentration of the scatterers (arborescent polymer molecules),  $P(q)$  is the single particle form factor (intraparticle interference), and  $S(q)$  is the structure factor (interparticle interference). In the single phase blends, the molecules are in the dilute concentration range and noninteracting, and only  $P(q)$  is observed. For the phase-separated G3 arborescent polymers in d-PVME at high temperature, it is expected that  $S(q)$  should play a role. The first peak observed in the scattering curve from the phase separated solution is due to the first neighbor interference (i.e.,  $S(q)$ ), as observed in many systems such as latex spheres and spherical block copolymers.<sup>60–64</sup> The second peak in the scattering curve has the same general shape and is in the same general  $q$  range as the peak observed in  $P(q)$  for the non-phase-separated samples. The interpretation of this peak as being associated with  $P(q)$  is also consistent with previous work on latex spheres and block copolymer systems.<sup>37,60,65–67</sup> From the position of the first peak the center-to-center distance between nearest-neighbor molecules was estimated using the relation  $d = (1.23 \times 2\pi)/q$ , which is valid for a structure controlled by two-body (noncrystalline) correlations.<sup>38,39</sup> This distance was found to be  $505 \pm 14 \text{ \AA}$ . From the position of the second peak, the diameter of a single molecule was estimated using the single particle scattering function derived from the power law function density profile (eq 5). The data in

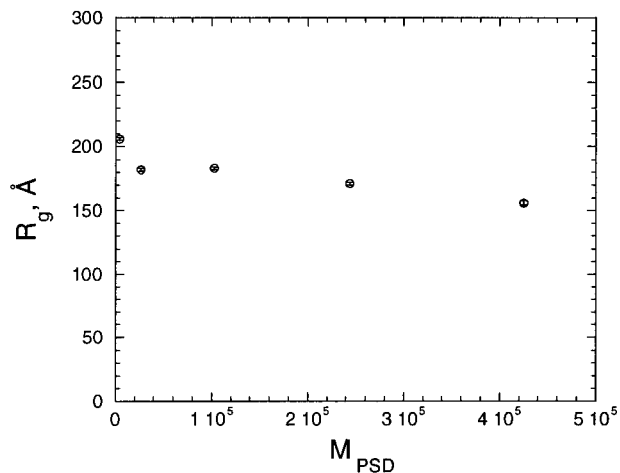


**Figure 10.**  $R_g$  of G3 arborescent polymer as a function of molecular mass of the matrix d-polystyrene. Note that error bars are on the same order of magnitude as the size of symbols in the plot.

the range  $q = 0.018\text{--}0.05 \text{ \AA}^{-1}$  were fitted to the scattering function calculated using the power law model with  $\alpha = 12$ .  $R_{\text{max}}$  was found to be  $232 \pm 4 \text{ \AA}$ , and the calculated density profile for phase-separated G3 polymer in d-PVME is shown in Figure 7. The error on the value of  $R_{\text{max}}$  was calculated from the errors in  $q$  based on the SANS instrument configuration. The diameter of a single molecule is  $d_{\text{max}} = 2R_{\text{max}} = 464 \pm 8 \text{ \AA}$ , which is smaller than the distance between nearest neighbors, indicating that the molecules are not quite in contact with each other. Using the power law density function given by eq 5, the radius of gyration was calculated from eq 7 and found to be  $R_g = (9/17)^{1/2} R_{\text{max}}$  (for  $\alpha = 12$ ). The  $R_g$  for a G3 arborescent polymer in d-PVME at  $115 \text{ }^\circ\text{C}$  (which is slightly inside the two-phase region of the phase diagram) calculated using this relation is  $169 \pm 3 \text{ \AA}$ . This is close to the  $R_g$  calculated for a sphere assuming the G3 molecule is collapsed to bulk density. This indicates that d-PVME is largely excluded from the interior of the arborescent molecules after phase separation occurs.

The  $R_g$  of G3 arborescent polymer molecules was studied as a function of the molecular mass of the linear d-PS matrix. The matrix molecular mass was varied from 4300 to 430 000 g/mol. The  $R_g$ , obtained using Guinier analysis, is plotted as a function of the molecular mass of the matrix polymer in Figure 10. Figure 10 shows that as the molecular mass of the matrix polymer increases, the  $R_g$  of the G3 polymer decreases. The largest decrease in  $R_g$  is observed when the matrix molecular mass increases from 4300 to 26 600 g/mol. There appears to be additional small decreases in  $R_g$  with further increases with molecular mass of the matrix polymer, but the magnitude is close to the errors of the measurements. The larger  $R_g$  observed for the lowest molecular mass matrix polymer indicates that the regions within the volume of the G3 arborescent polymer are limited in size and shape and only accessible to the shortest chains. The configurational entropy penalty for higher molecular mass polymers to penetrate the coil of the arborescent polymer is too great compared to the (relatively small) gain in mixing energy.

## Conclusions

The radius of gyration of arborescent polymers decreases in going from solutions to polymer blends. The

size of arborescent polymers in deuterated polystyrene is smaller than in deuterated poly(vinyl methyl ether). The scaling exponent for  $R_g \sim M^\nu$  is found to be  $\nu = 0.28 \pm 0.02$  in d-PVME and  $\nu = 0.26 \pm 0.06$  in d-PS, which indicates that arborescent segment density is increasing as a function of generation. The scattering curve calculated using a power law model is in reasonable agreement with the measured scattering. The value of  $\alpha$  in the power law model is largest for arborescent polymers in deuterated polystyrene, and the sequential density calculated from the molecular mass divided by the volume of coil of the arborescent polymer in deuterated polystyrene is found to be close to bulk density. This indicates that the molecules are essentially non-interpenetrating and exclude the linear matrix chains. For G3 polymer in deuterated poly(vinyl methyl ether), two peaks in the  $I(q)$  versus SANS data are observed above the phase separation temperature ( $105 \text{ }^\circ\text{C}$ ), and the  $R_g$  of the phase-separated sample decreases by about 21% upon phase separation. In the two phase blends, G3 polymer molecules are found to be not in contact with each other.

**Acknowledgment.** This work has benefited from the use of the 30 m NIST-NG3 instrument at the Center for Neutron Research of the National Institute of Standards and Technology. It is based upon activities supported by the National Science Foundation under Agreement DMR-9423101. We acknowledge the support of the National Institute of Standards and Technology, U.S. Department of Commerce, in providing the neutron research facilities used in this experiment. The authors thank Dr. J. Barker and Dr. S. Klein at NIST for help with the SANS experiments and data analysis. This material is based upon work supported in part by the U.S. Army Research Office under Contract 35109-CH. M. Gauthier thanks the Natural Sciences and Engineering Research Council of Canada for financial support.

## References and Notes

- (1) Tomalia, D. A.; Baker, H.; Dewald, J.; Hall, M.; Kalos, G.; Martin, S.; Roeck, J.; Ryder, J.; Smith, P. *Polym. J.* **1985**, *17*, 117.
- (2) Tomalia, D. A.; Naylor, A. M.; Goddard, W. A. *Angew. Chem., Int. Ed. Engl.* **1990**, *29*, 138.
- (3) Tomalia, D. A.; Hedstrand, D. M.; Wilson, L. R. *Encyclopedia of Polymer Science and Engineering; Index Volume*, 2nd ed.; John Wiley & Sons: New York, 1990; p 46.
- (4) Mourey, T. H.; Turner, S. R.; Rubinstein, M.; Fréchet, J. M. J.; Hawker, C. J.; Wooley, K. L. *Macromolecules* **1992**, *25*, 2401.
- (5) Kim, Y. H.; Webster, O. W. *J. Am. Chem. Soc.* **1990**, *112*, 4592.
- (6) Turner, S. R.; Voit, B. I.; Mourey, T. H. *Macromolecules* **1993**, *26*, 4617.
- (7) Gauthier, M.; Möller, M. *Macromolecules* **1991**, *24*, 4548.
- (8) Gauthier, M.; Möller, M.; Burchard, W. *Macromol. Symp.* **1994**, *77*, 43.
- (9) Gauthier, M.; Tichagwa, L.; Downey, J. S.; Gao, S. *Macromolecules* **1996**, *29*, 519.
- (10) Sheiko, S. S.; Gauthier, M.; Möller, M. *Macromolecules* **1997**, *30*, 2343.
- (11) Frank, R. S.; Merkle, G.; Gauthier, M. *Macromolecules* **1997**, *30*, 5397.
- (12) Gauthier, M.; Li, W.; Tichagwa, L. *Polymer* **1997**, *38*, 6363.
- (13) Gauthier, M.; Chung, J.; Choi, L.; Nguyen, T. T. *J. Phys. Chem. B* **1998**, *102*, 3138.
- (14) Lue, L.; Prausnitz, J. M. *Macromolecules* **1997**, *30*, 6650.
- (15) Boris, D.; Rubinstein, M. *Macromolecules* **1996**, *29*, 7251.
- (16) Choi, S.; Briber, R. M.; Bauer, B. J.; Topp, A.; Gauthier, M.; Tichagwa, L. *Macromolecules* **1999**, *32*, 7879.

- (17) Flory, P. J. *Principles of Polymer Chemistry*; Cornell University Press: Ithaca, NY, 1953.
- (18) Zimm, B. H.; Stockmayer, W. H. *J. Chem. Phys.* **1949**, *17*, 1301.
- (19) de Gennes, P. G.; Hervet, H. *J. Physiol. Lett.* **1983**, *44*, L351.
- (20) Stauffer, D. *Phys. Rep.* **1979**, *54*, 1.
- (21) Stauffer, D. *Pure Appl. Chem.* **1981**, *53*, 1479.
- (22) Stauffer, D.; Coniglio, A.; Adam, M. *Adv. Polym. Sci.* **1982**, *44*, 103.
- (23) Lescanec, R. L.; Muthukumar, K. *Macromolecules* **1990**, *23*, 2280.
- (24) Mansfield, M. L.; Klushin, L. I. *Macromolecules* **1993**, *26*, 4262.
- (25) Mansfield, M. L. *Polymer* **1994**, *35*, 1827.
- (26) Murat, M.; Grest, G. S. *Macromolecules* **1996**, *29*, 1278.
- (27) Stechemesser, S.; Eimer, W. *Macromolecules* **1997**, *30*, 2204.
- (28) Boris, D.; Rubinstein, M. *Macromolecules* **1996**, *29*, 7251.
- (29) Prosa, T. J.; Bauer, B. J.; Amis, E. J.; Tomalia, D. A.; Scherrenberg, R. *J. Polym. Sci.* **1997**, *35*, 2913.
- (30) Prosa, T. J.; Bauer, B. J.; Amis, E. J. To be submitted.
- (31) Pötschke, D.; Ballauff, M.; Lindner, P.; Fischer, M.; Vögtle, F. *Macromolecules* **1999**, *32*, 4079.
- (32) Certain commercial materials and equipment are identified in this paper in order to specify adequately the experimental procedure. In no case does such identification imply recommendation by the National Institute of Standards and Technology nor does it imply that the material or equipment identified is necessarily the best available for this purpose.
- (33) Hawker, C. J.; Barclay, G. G.; Orellana, A.; Dao, J.; Devonport, W. *Macromolecules* **1996**, *29*, 5245.
- (34) Bauer, B. J.; Hanley, B.; Muroga, Y. *Polym. Commun.* **1989**, *30*, 19.
- (35) Liu, X. Ph.D. Dissertation, University of Maryland, College Park, MD, 1995.
- (36) *NG3 and NG7 30-meter SANS Instruments Data Acquisition Manual*, National Institute of Standards and Technology Cold Neutron Research Facility, 1996.
- (37) Glinka, C. J.; Barker, J. G.; Hammouda, B.; Krueger, S.; J. Moyer, J. J.; Orts, W. J. *J. Appl. Crystallogr.* **1998**, *31*, 430.
- (38) Guinier, A.; Fournet, G. *Small Angle Scattering of X-Rays*; Wiley: New York, 1955.
- (39) Guinier, A. *X-Ray Diffraction*; W. H. Freeman and Company: San Francisco, 1963.
- (40) Horii, F.; Hirai, A.; Kitamaru, R. *Macromolecules* **1986**, *19*, 932.
- (41) Higgins, J. S.; Benoit, H. C. *Polymers and Neutron Scattering*; Oxford Science Publications: New York, 1994.
- (42) Nishi, T.; Kwei, T. K. *Polymer* **1975**, *16*, 285.
- (43) Private discussions with Dr. Martin Neese.
- (44) Feigin, L. A.; Svergun, D. I. *Structure Analysis by Small Angle X-Ray and Neutron Scattering*; Plenum Press: New York, 1987.
- (45) Barker, J. G.; Pedersen, J. S. *J. Appl. Crystallogr.* **1995**, *28*, 105.
- (46) Mildner, D. F. R.; Carpenter, J. M. *J. Appl. Crystallogr.* **1984**, *17*, 249.
- (47) Glatter, O. *Modern Methods of Data Analysis in Small Angle Scattering and Light Scattering*; Kluwer Academic Publishers: Norwell, MA, 1995.
- (48) Choi, S.; Liu, X.; Briber, R. M. *J. Polym. Sci., Part B* **1998**, *36*, 1.
- (49) Briber, R. M.; Bauer, B. J.; Hammouda, B. *J. Chem. Phys.* **1994**, *101*, 2592.
- (50) Han, C. C.; Bauer, B. J.; Clark, J. C.; Muroga, Y.; Matsushita, Y.; Okada, M.; Tran-cong, Q.; Chang, T.; Sanchez, I. C. *Polymer* **1988**, *29*, 2002.
- (51) Williams, C.; Brochard, F.; Frisch, H. L. *Annu. Rev. Phys. Chem.* **1981**, *32*, 433.
- (52) Chu, B.; Wang, J.; Grosberg, A. Y. *Macromolecules* **1995**, *28*, 180.
- (53) Sariban, A.; Binder, K. *Makromol. Chem.* **1988**, *189*, 2357.
- (54) Di Marzio, E. A.; Briber, R. M. *Macromolecules* **1995**, *28*, 4022.
- (55) Swislow, G.; Sun, S.; Nishio, I.; Tanaka, T. *Phys. Rev. Lett.* **1980**, *44*, 796.
- (56) Chu, B.; Wang, J. *Macromolecules* **1989**, *22*, 380.
- (57) Park, I. H.; Wang, Q. W.; Chu, B. *Macromolecules* **1987**, *20*, 1965.
- (58) Chu, B.; Park, I. H.; Wang, Q. W.; Wu, C. *Macromolecules* **1987**, *20*, 2833.
- (59) Bauer, D. R.; Ullman, R. *Macromolecules* **1980**, *13*, 392.
- (60) Dingenouts, N.; Ballauff, M. *Langmuir* **1999**, *15*, 3283.
- (61) Hashimoto, T.; Tsukahara, Y.; Kawai, H. *Macromolecules* **1981**, *14*, 708.
- (62) Sasaki, K.; Hashimoto, T. *Macromolecules* **1984**, *17*, 2818.
- (63) Bates, F. S. *Macromolecules* **1984**, *17*, 2607.
- (64) Bates, F. S.; Dierker, S. B.; Wignall, G. D. *Macromolecules* **1986**, *19*, 1938.
- (65) Hashimoto, T.; Fujimura, M.; Kawai, H. *Macromolecules* **1980**, *13*, 1660.
- (66) Bates, F. S.; Cohen, R. E.; Berney, C. V. *Macromolecules* **1982**, *15*, 589.
- (67) Bates, F. S.; Berney, C. V.; Cohen, R. E. *Macromolecules* **1983**, *16*, 1101.

MA000160V